Wintertime Arctic Sea Spray Aerosol Composition Controlled by Sea Ice Lead Microbiology

Rachel M. Kirpes,[†] Daniel Bonanno,[‡] Nathaniel W. May,[†] Matthew Fraund,[‡] Anna J. Barget,[†] Ryan C. Moffet,[‡,⊥] Andrew P. Ault,*[,†,§] and Kerri A. Pratt*[,†,‖]

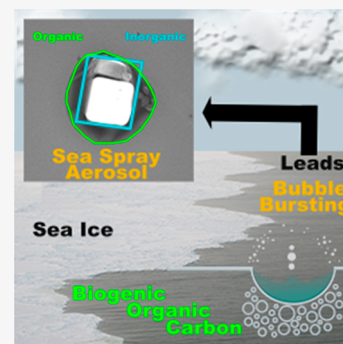[†]Department of Chemistry, University of Michigan, Ann Arbor, Michigan 48109, United States
[‡]Department of Chemistry, University of the Pacific, Stockton, California 95211, United States
[§]Department of Environmental Health Sciences, University of Michigan, Ann Arbor, Michigan 48109, United States
[‖]Department of Earth & Environmental Sciences, University of Michigan, Ann Arbor, Michigan 48109, United States

S Supporting Information

ABSTRACT: The Arctic is experiencing the greatest warming on Earth, as most evident by rapid sea ice loss. Delayed sea ice freeze-up in the Alaskan Arctic is decreasing wintertime sea ice extent and changing marine biological activity. However, the impacts of newly open water on wintertime sea spray aerosol (SSA) production and atmospheric composition are unknown. Herein, we identify SSA, produced locally from open sea ice fractures (leads), as the dominant aerosol source in the coastal Alaskan Arctic during winter, highlighting the year-round nature of Arctic SSA emissions. Nearly all of the individual SSA featured thick organic coatings, consisting of marine saccharides, amino acids, fatty acids, and divalent cations, consistent with exopolymeric secretions produced as cryoprotectants by sea ice algae and bacteria. In contrast, local summertime SSA lacked these organic carbon coatings, or featured thin coatings, with only open water nearby. The individual SSA composition was not consistent with frost flowers or surface snow above sea ice, suggesting that neither hypothesized frost flower aerosolization nor blowing snow sublimation resulted in the observed SSA. These results further demonstrate the need for inclusion of lead-based SSA production in modeling of Arctic atmospheric composition. The identified connections between changing sea ice, microbiology, and SSA point to the significance of sea ice lead biogeochemistry in altering Arctic atmospheric composition, clouds, and climate feedbacks during winter.

INTRODUCTION

With rapidly declining Arctic sea ice extent and increasing open water,[1] sea spray aerosol (SSA) emissions are predicted to be increasing.[2] Notably, even wintertime coastal sea ice in the Arctic is drastically decreasing as a result of sea ice freeze-up delays in the Bering, Chukchi, Barents, and East Greenland Seas.[3] Thick multiyear sea ice is being replaced by thinner first-year ice, which is more susceptible to fracturing and forming leads, open areas of water surrounded by ice.[4] During Arctic winter, fresh (nascent) SSA comprises a significant aerosol fraction: up to 40% and 25% of supermicron and submicron aerosol mass,[5] and up to 90% and 50% of supermicron and submicron aerosol number, respectively.[6] While wintertime SSA was previously thought to primarily be transported long distances to the Arctic,[5] recent work showed that leads contribute to local Arctic SSA emissions year-round.[7]

SSA composition reflects the surface seawater,[8,9] which is expected to be altered by changing marine productivity in the warming Arctic.[10] In the open ocean, SSA particles are primarily generated by wave breaking processes resulting in bubble bursting at the ocean surface, creating film and jet drops that form SSA.[11] Wind-driven wave breaking processes also produce SSA in leads, at lower concentrations than in open water due to the reduced fetch.[7,12−14] Supermicron SSA

particles (>1 μm; 2 μm number mode) are primarily inorganic salts but can also contain organic matter.[11] These inorganic salts are hygroscopic, with a high efficiency of forming cloud droplets.[11] Submicron SSA particles (<1 μm; ∼200 nm number mode) can be significantly enriched in organic matter (>50%, by mass) in comparison to bulk seawater.[9,15] SSA organic coatings can inhibit heterogeneous reactions of trace gases, inhibiting particulate chloride depletion, and impacting trace gas budgets and atmospheric composition.[16] However, recent work has shown that surfactant coatings on SSA can actually enhance certain reactions.[17] Laboratory studies with ambient seawater also show suppression of SSA hygroscopicity by certain organics, potentially altering cloud condensation nuclei (CCN) activity.[18,19] Enhanced cloud ice nucleation efficiency is observed for Arctic seawater, suggesting a contribution of SSA to cloud ice formation.[20−22] Despite important climate implications for cloud formation and phase, and associated longwave radiative forcing,[23] limited knowledge exists regarding ambient SSA organic coatings and the transfer of marine biogenic organics to the particle phase,[8] particularly for Arctic winter.
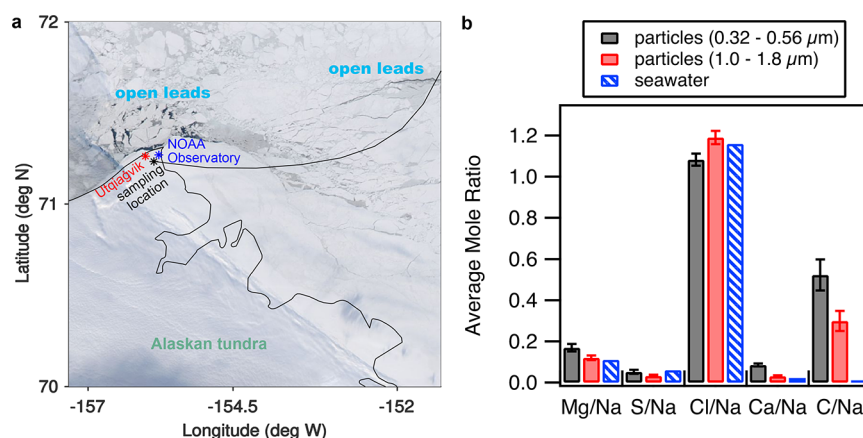
Figure 1. Observations of open leads and wintertime SSA composition. (a) MODIS satellite imagery from February 26, 2014 (NASA Worldview) shows open leads near Utqiaġvik, Alaska. Locations of the town, NOAA Observatory, and aerosol sampling location are shown. The black line shows 8 h of a NOAA HYSPLIT backward air mass trajectory (February 26, 2014 20:00 AKST; 50 m altitude at the sampling site) passing over the closest open leads before arriving at the site. The air mass traveled ∼60 km from open leads to the northeast. (b) CCSEM-EDX average individual sub- and supermicron SSA particle elemental mole ratios compared to literature values for seawater.[40] Error bars denote 95% confidence intervals.

While previous studies have primarily focused on marine biological activity during the Arctic summer, recent work has shown that microalgal growth is initiated prior to the spring phytoplankton bloom period and under extremely low light conditions under sea ice,[24,25] including during sea ice covered periods.[26,27] The sea ice algae and bacteria present produce exopolymeric substances (EPS) as a cryoprotectant,[28,29] with phytoplankton releasing it extensively.[30] Production of EPS is critical to sea ice algae survival through the winter.[31,32] Indeed, EPS have been observed in winter in both sea ice[27,33] and seawater.[33] In the high Arctic, aerosols produced from laboratory bubbling experiments in the summer pack ice showed enrichment of EPS-derived polysaccharides relative to the seawater surface microlayer (SML),[34] with microgels and EPS-derived compounds also observed in the ambient aerosols.[35] However, there is a critical knowledge gap in our understanding of wintertime aerosol sources and composition in the changing Arctic,[6] particularly with increasing open water.[3] Therefore, atmospheric particles were collected near Utqiaġvik, Alaska, in January and February 2014 for individual particle measurements of morphology, elemental composition, spatial distribution and quantity of organic material, and organic functional groups associated with marine biogenic compounds. This novel detailed characterization of individual SSA, and associated organic material, significantly improves our knowledge of Arctic SSA and connections to sea ice microbiology at a time of year when few aerosol measurements exist.

■ RESULTS AND DISCUSSION

SSA Production from Open Leads. Atmospheric particles were collected at Utqiaġvik, Alaska, an Arctic coastal site during January and February 2014. The sampling site was located ∼5 km inland and ∼60 km downwind of the sea ice leads (Figure 1). A total of 1691 individual particles (0.32−0.56 and 1.0−1.8 μm aerodynamic diameter, d_a) from six sample periods (January 24−27 and February 26−27, 2014) were analyzed by computer-controlled scanning electron microscopy with energy dispersive X-ray spectroscopy (CCSEM-EDX) to determine individual particle morphology and elemental composition. Nearly all (86% of submicron and >99% of supermicron particles, by number) of the collected

particles were identified as SSA (Figure S1), consistent with our previous measurements during this study.[6] For the samples herein, 75%, by number, of SSA particles were classified as nascent, based on the presence of Na and Cl in ratios similar to seawater.[6] An additional 25%, by number, of the SSA particles were classified as partially aged based on the simultaneous enrichment of S and/or N and depletion of Cl, relative to seawater, and consistent with long-range transport.[6] Given local Arctic production of nascent SSA,[7] the sources and composition of the nascent SSA are the focus of this study.

SSA production from open leads is supported by the presence of nearby open leads on all sampling days; the closest upwind leads were within 4 h of atmospheric transport time to the sampling site, according to satellite and local sea ice imagery, combined with backward air mass trajectories (Figure 1, Figure S2). In recent years, open leads have persisted throughout the winter near Utqiaġvik.[7,36−39] Consistent with lead-based SSA production at elevated wind speeds (>4 m s^{-1}),[7,12−14] all samples were collected during periods of wind speeds greater than or equal to 4 m s^{-1} (average wind speeds of 6−12 m s^{-1}), and four samples were collected during sustained periods of high wind speeds (6−17 m s^{-1}) (Table S1). While nascent SSA particles were observed in all samples, the samples with the greatest number fractions of nascent SSA relative to partially aged SSA had the greatest near-surface (<70 m above sea level) air mass transport over the ice-fractured Arctic Ocean.[6] All samples had air mass back trajectories influenced by the central Arctic Ocean, as shown in previous work.[6] Average elemental mole ratios of S/Na and Cl/Na for individual sub- and supermicron SSA particles were similar to seawater ratios (Figure 1), as discussed in the Supporting Information.[40] These elemental ratios have been observed previously for laboratory-generated SSA[9] and are consistent with aerosol production from the nearby open leads.[7,13] Based on the low concentrations of sulfur- and nitrogen-containing trace gases in the winter Arctic,[41] nascent SSA in the sub- and supermicron size ranges could be transported from these leads with little influence from multiphase aging reactions altering particle chemical composition. At high wind speeds, blowing snow and frost flowers have also been hypothesized to result in lofted SSA.[42,43] However, the measured sub- and supermicron SSA elemental

ratios are not consistent with simultaneously measured sea ice surface snow or previous measurements of frost flowers (Table S3),[44] as discussed in the Supporting Information. Particles produced by sublimation of blowing snow or aerosolization of frost flowers are suggested to be distinguished from nascent SSA based on chemical composition, characterized by sulfur depletion compared to seawater, due to mirabilite precipitation impacting brine migration through frost flowers and snow above sea ice.[44−46] However, during this study, there was no dependence of individual SSA S/Na mole ratios on wind speed (Figure S3), a trend which would be expected for a wind-dependent blowing snow or frost flower source. This is consistent with recent work demonstrating that frost flowers are unlikely to produce aerosol under high wind conditions.[47,48]

Overall, the measured individual SSA particles were closest in composition to seawater and the measured tundra surface snow (Table S3), as discussed in the Supporting Information. This is in part due to the high variability in the measured values of the tundra surface snow (Table S3), but it is also consistent with SSA deposition to the tundra snowpack following transport from the upwind sea ice region containing leads. The submicron SSA particles showed calcium and magnesium enrichment above the seawater ratio (Figure 1 and Table S3), consistent with the presence of EPS as assembled gels bound by divalent cations (Ca^{2+}; Mg^{2+}).[49,50] As discussed in the following sections, the observed organic coatings, size-dependent trends in C/Na ratios, and organic composition further support the presence of EPS and a wave-breaking seawater source for the observed SSA. Overall, the measured nascent SSA composition is consistent with SSA production from local open sea ice leads, rather than blowing snow, as previously observed through multiyear bulk aerosol measurements at Utqiaġvik from fall−spring.[7] Our observation herein further highlights the year-round nature of SSA emissions in the Alaskan Arctic from open water, including leads.

Abundance of Organic Material in SSA. Carbon was observed in over 98% of the nascent SSA particles, by number, and was typically observed as a coating on the salt particles (Figure 2a,b). Individual SSA particles with similar morphology and organic coatings were previously observed during spring in the Norwegian Sea.[51] Previous bulk aerosol measurements at Utqiaġvik also showed organic mass to be correlated with sea salt during winter.[52] We demonstrate through single-particle analyses that these organics are present as sea salt coatings. The individual nascent SSA particles contained substantial amounts of carbon, with average atomic percentages of carbon of 15 ± 8% and 6 ± 5% for submicron and supermicron SSA, respectively. These particles were also significantly enriched in carbon relative to seawater, with C/Na ratios of 0.52 ± 0.07 and 0.30 ± 0.05 for submicron and supermicron SSA, respectively, compared to 0.01 for seawater (Figure 1).[40] Significant supermicron SSA C/Na enrichments (0.8 ± 0.3) have also previously been observed in the Antarctic during winter.[53] Analysis of 150 SSA particles by scanning transmission X-ray microscopy with near edge X-ray absorption fine structure spectroscopy (STXM-NEXAFS) showed over 90%, by number, contained organic carbon (detected as the −COOH functional group), consistent with the CCSEM-EDX results (Table S2). Notably, no organic gel-like particles[54] without inorganic salts were observed. For all particles measured here (>100 nm), all submicron organic carbon was either coating SSA particles (Figures S1 and S4),
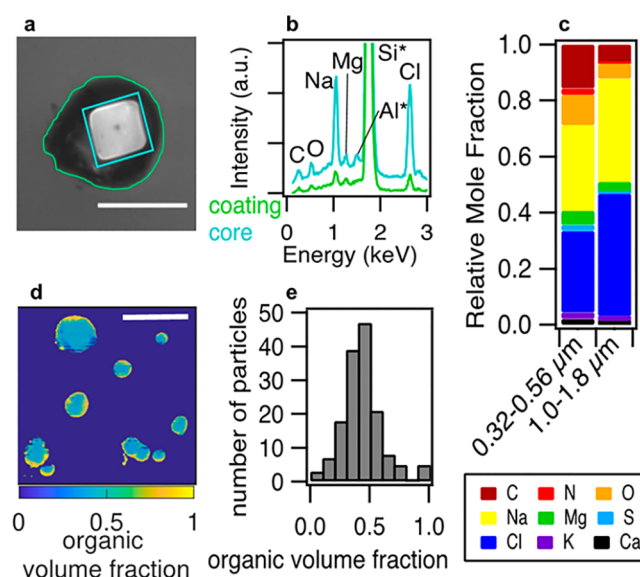

Figure 2. Organic coatings observed on wintertime sea spray aerosol (SSA) particles. (a) SEM image with a 3 μm scale bar shown and (b) EDX spectra of a representative SSA particle with a cubic salt core (blue) and organic coating (green). *Al and Si signal contributions are from the sampler holder and substrate, respectively. (c) Average relative elemental (mole) fractions for all 773 submicron and 918 supermicron nascent SSA particles (CCSEM-EDX). (d) Representative STXM-NEXAFS image showing organic volume fraction spatial distribution within individual SSA particles, with a 5 μm scale bar shown. (e) Histogram of 150 individual SSA particle organic volume fractions (STXM-NEXAFS).

consistent with midlatitude SSA studies,[9] or internally mixed with anthropogenic secondary sulfate.[6] Given the calcium enrichment in the wintertime submicron SSA and thick organic coatings, these results are consistent with assembled gel coatings surrounding inorganic sea salt cores.

The average individual SSA organic volume fractions for each sample ranged from 0.41 to 0.47 (Table S2), with little variation across the time periods and particle size ranges analyzed. As shown in Figure 2, the majority of SSA particles (71%, by number) had organic volume fractions between 0.3 and 0.5, consistent with organic volume fractions (0.2−0.5) observed for SSA produced in midlatitude algal bloom mesocosm experiments.[18,55] Notably, 26% of the SSA particles analyzed by STXM-NEXAFS had organic volume fractions of 0.5 or greater. Particles with lower organic volume fractions (<0.2) were inorganic salts with thin organic coatings, whereas particles with higher organic volume fractions (>0.2) had thick organic coatings around inorganic salt cores (Figure 2). Based on the average individual SSA particle measured organic volume fraction of 0.45, the average coating thickness was calculated to be ∼0.04 and ∼0.13 μm for the median submicron (0.44 μm) and supermicron (1.4 μm) particle aerodynamic diameters analyzed, respectively.

For comparison to the wintertime SSA described herein, SSA particles were also collected at the same site near Utqiaġvik during September 2015, when the nearest sea ice was >400 km upwind. Meteorological conditions, including wind speeds, were similar during the winter (Table S1) and summer[56] studies. To compare the enrichment of organics in SSA between winter and summer, individual SSA particle carbon/sodium (C/Na) ratios were determined by SEM-EDX for ∼150 particles. Overall, the winter SSA particles had

statistically greater C/Na ratios (range 0.2–1.2; median 0.6) compared to the summer SSA particles (range 0.1–0.3; median 0.2) (Figure 3a). The higher carbon content observed
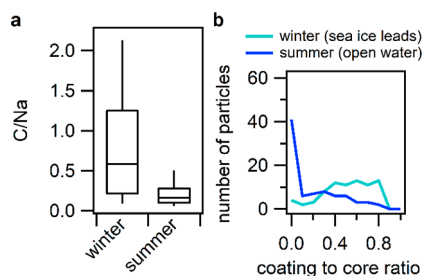

Figure 3. Comparison of SSA organic coatings observed in winter and summer. (a) Box and whisker plot (90th/10th percentiles, 75th/25th percentiles, and medians) of C/Na ratios determined for individual SSA particles in winter and summer. C/Na distributions for winter and summer SSA particles were significantly different (Kolmogorov–Smirnov test, $p = 2.0010 \times 10^{-27}$). (b) Histogram of measured organic coating to salt core diameter ratios determined from SEM images for winter (77 particles) and summer (82 particles) SSA particles on aluminum foil substrates. A two-sample Kolmogorov–Smirnov test showed that the two distributions were not from the same underlying population ($p = 5.28 \times 10^{-14}$).

in the winter SSA is consistent with the measured ratios of organic coating thickness relative to the salt core diameter, as determined by SEM-EDX, which showed statistically thicker coatings for winter compared to the summer SSA particles (Figure 3b). The coating thickness to salt core diameter analysis of the winter SSA is in agreement with the thick organic coatings observed by STXM-NEXAFS (Figure 2d,e). 78% of winter SSA particles had coating to core ratios greater than 0.4, compared to the summer SSA samples, which showed 57%, by number, to have coating to core ratios of 0.1 or less (Figure 3b). Together these measurements show that the organic coatings of winter SSA particles, sampled near Utqiaġvik, Alaska, were much thicker than the organic coatings

on the summer SSA particles, indicating an important unique source of SSA organic content during winter. This is consistent with previous work, showing through bulk measurements that organic mass was higher in the winter near Utqiaġvik and correlated with sea salt aerosol.[52] Given the lack of nearby sea ice in the summer near Utqiaġvik, we suggest that sea ice algae, bacteria, and phytoplankton contribute to the thick SSA organic coatings observed in winter when these micro-organisms use EPS in great quantities as a cryoprotectant.[27−31] Therefore, the molecular composition of the winter SSA organic content was investigated to probe this hypothesis.

Molecular Characterization of SSA Organic Content. To determine the chemical composition of the SSA organic coatings, 88 submicron and 212 supermicron individual SSA particles were analyzed with Raman microspectroscopy. Similar organic composition was observed for the sub- and super-micron SSA particles, and for all sampling periods. The organic compound classes present included saccharides (monosaccharides, polysaccharides, and lipopolysaccharides), short-chain fatty acids (and dicarboxylic acids), surfactant long-chain fatty acids (and lipids and phospholipids), and amino acids, with representative individual SSA spectra shown in Figure 4a. Raman peak assignments and χ^2 fitting with SML standards are given in the Supporting Information (Table S4 and Figure S7).[19] Fluorescence microscopy confirmed the presence of fluorescing biological organic material[57] in the individual wintertime SSA particles (Figure S5).

Saccharides and short-chain fatty acids were the most commonly observed marine biogenic organic compound classes present in the SSA particles, with 49% of individual SSA particle Raman spectra containing at least one saccharide (Figure 4b). Saccharides observed, particularly xylose, fucose, and glucose, are major components of EPS.[34,51,54] The monosaccharides observed are similar to that of the SML, as well as bulk ambient aerosol and aerosols produced from laboratory bubbling experiments in the summer high Arctic pack ice.[34,35] In prior studies during spring over the Norwegian Sea, individual SSA particles with organic coatings were
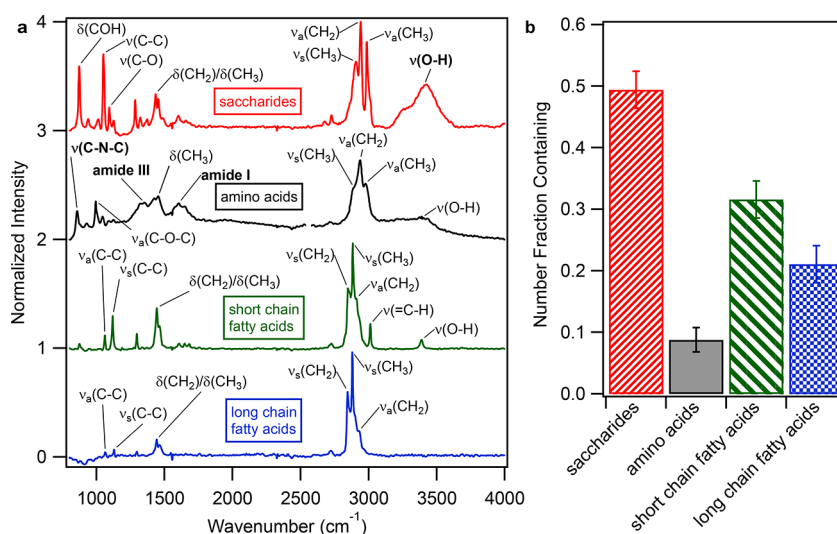

Figure 4. Marine-derived organic compound types observed in individual wintertime SSA particles. (a) Raman spectra of four representative individual SSA particles matching marine-derived saccharides ($\chi^2 = 0.013$), amino acids ($\chi^2 = 0.011$), short-chain fatty acids ($\chi^2 = 0.003$), and long-chain fatty acids ($\chi^2 = 0.0005$), respectively. (b) Number fractions (and associated standard errors) of 300 individual SSA particles containing saccharides, amino acids, short-chain fatty acids, and/or long-chain fatty acids. Each SSA particle Raman spectrum was allowed to be fitted to up to two organic compound types, following the method of Cochran et al.[19]

characterized by STXM-NEXAFS as having a prominent carboxylic acid peak (as observed here), which was attributed to polysaccharides from the SML.[51] Saccharides have also previously been observed in bulk Arctic aerosol samples during spring over the Norwegian Sea,[58,59] summer in the Canadian[60] and high[35] Arctic, and winter near Utqiaġvik.[52]

Similar to saccharides, long-chain fatty acid surfactants and amino acids were also commonly observed in the winter SSA coatings. 32% of individual SSA particle Raman spectra contained at least one short-chain fatty acid, while long-chain fatty acids and amino acids were present in 21% and 9% of SSA particles, by number, respectively (Figure 4). Amino acids and fatty acids have previously been observed in the SML of open leads in the summer high Arctic[61,62] and in bulk ambient aerosols during spring−summer in the Canadian Arctic,[60,63] and during spring−fall at Svalbard.[64,65] Notably, all SSA particles containing amino acids also contained saccharides, and most particles (75%, by number) containing one short-chain fatty acid also contained a saccharide signature. Only 33% of particles matching saccharides did not contain any other organic type. For the particles containing surfactants, including long-chain fatty acids, 40% matched only long-chain fatty acids, while the other 60% also contained short-chain fatty acids or saccharides. Since saccharides, amino acids, and fatty acids are EPS components,[34,51,54] the presence of these compounds together in the individual SSA organic coatings is consistent with incorporation during the bubble bursting aerosol formation process due to enrichment in the SML of sea ice leads.

Atmospheric Implications. In this study, we identified abundant wintertime SSA thickly coated by marine biogenic organic carbon, with signatures consistent with EPS produced as a cryoprotectant by sea ice algae and bacteria. This study was conducted soon after polar sunrise, in line with recent unexpected evidence of sea ice biological activity under low light conditions in the Arctic.[24,32,66] The measured SSA chemical composition is consistent with Arctic lead-based aerosol production, illustrating the connections between sea ice fracturing, marine biological activity, EPS, and SSA production in the winter Arctic. This finding further highlights the year-round nature of Arctic SSA emissions and identifies a need for further studies of wintertime sea ice microbiology in the Alaskan Arctic. The observed SSA particles were similar in composition to seawater and demonstrated a size dependence in organic enrichment and coatings, as previously observed for particles produced via bubble bursting at the ocean surface. Open sea ice leads enriched in EPS are identified as leading to organic enrichment in wintertime SSA. Alternative hypotheses for SSA production, including blowing snow and frost flowers,[42,43] were determined to be unlikely sources, based on the individual particle composition, and the consistency of the observed size-dependent trends and composition to those in lower latitude SSA.[8,9] To our knowledge, Arctic chemical transport modeling has not yet included leads as a possible SSA source, but our findings, combined with those from the summertime High Arctic pack ice,[12,13] demonstrate the need for consideration of lead-based SSA production in future modeling studies.

The Arctic is currently changing at an unprecedented rate,[1] with winter warming events rapidly increasing.[23] Resulting sea ice loss is expanding first year sea ice,[1] which is prone to fracturing and expected to result in increasing SSA emissions.[2] Notably, delayed sea ice freeze-up in the Bering, Chukchi,

Barents, and East Greenland Seas is dramatically decreasing sea ice extent in these regions[3] and increasing marine biological activity,[10,25,32] impacting SSA emissions and organic content. SSA organic coatings can reduce reactivity toward trace gases, such as nitric acid, thereby impacting atmospheric composition[16] and Arctic haze formation.[67] Organic coatings can also reduce SSA hygroscopicity[19] and CCN efficiency[18] and may contribute to cloud ice nucleation,[20] which impacts cloud formation in the often CCN-limited Arctic.[68] Cloud-aerosol feedbacks are especially important in the Arctic winter when there is little to no direct solar radiation; clouds trap longwave radiation near the surface and contribute to warming, with increasing sensitivity to clouds projected for the fall—winter.[23,69] Therefore, additional studies are critical to quantify and upscale the details of, and connections between, changing Arctic microbiology, EPS production, SSA production, atmospheric composition, and cloud feedbacks in the winter.

■ METHODS

Atmospheric particles were collected near Utqiaġvik (Barrow), AK during January 24−27 and February 26−27, 2014, at a tundra site ~5 km inland (71.17° N, 156.38° W), at a sampling height ~1.5 m above ground level. Sample collection times and meteorological parameters, measured at the NOAA Barrow Observatory located 5 km upwind across flat tundra, are provided in the Supporting Information (Table S1). Particles were collected using a 10-stage rotating micro-orifice uniform deposit impactor (MOUDI, model 110, MSP Corp.) sampling at 30 L min^{-1} through a 10 μm cut point cyclone (URG-2000-30EA). Particles were impacted on silicon substrates (Ted Pella, Inc.) and aluminum foil substrates (MSP Corp.) for analysis by SEM-EDX, quartz substrates (Ted Pella, Inc.) for analysis by Raman microspectroscopy, and transmission electron microscopy (TEM) grids (Carbon Type-B Formvar film copper grids, Ted Pella, Inc.) for analysis by STXM-NEXAFS. Samples were stored frozen at −15 °C prior to analysis. Particles collected on two MOUDI stages with 50% size cuts of 1.8 and 0.56 μm d_a, respectively, were analyzed in this work.

For comparison to the winter SSA SEM-EDX analysis, atmospheric particles were collected at the same location during September 15−16 and 23−24, 2015. Samples were collected for ~8 h each using a three-stage microanalysis particle sampler (MPS, California Measurements, Inc.) with aluminum foil substrates (MSP Corp.) on stages 1 and 2 (2.8−5.0 and 0.50−2.8 μm, respectively) and TEM grids (Carbon Type-B Formvar film copper grids, Ted Pella, Inc.) on stage 3 (0.07−0.40 μm). Additional sampling details are described by Gunsch et al.[56]

Individual particle analysis by computer-controlled SEM-EDX (CCSEM-EDX) was conducted using an FEI Nova 200 nanolab SEM/FIB operating at 15 kV accelerating voltage with a secondary electron detector. X-ray spectra from elements with atomic numbers greater than Be (Z > 4) were detected with an EDX detector (EDAX, Inc.). For each substrate collected during the six winter sample periods, ~75−150 particles were analyzed by CCSEM-EDX to measure individual particle morphology (particle projected area, average diameter, and perimeter) and relative abundance of the following elements: C, N, O, Na, Mg, S, Cl, K, Ca, Ti, Fe, and Zn.[70] EDX has previously been shown to quantitatively reproduce SSA elemental ratios.[9] Carbon was below the detection limit on the Si wafer without particles, indicating that substrate

contamination from C was not present in the particle spectra (Figure S6). EDX can be slightly less sensitive to C, N, and O, compared to heavier elements, such that the C, N, and O percentages reported here represent lower limits.[70] Particle types present were determined by k-means clustering of the EDX spectra using a previously established method.[71]

SEM images of particles collected on aluminum foil substrates were used to measure individual SSA particle coating to core ratios for 77 winter particles from January 24, 2014, as well as 82 summer SSA particles collected at the same sampling location on September 16, 2015.[56] SEM images of each sample were analyzed using ImageJ to determine the inorganic (bright core) and organic (dark coating) areas of each individual SSA particle (Figure S8). The coating (primarily organic) to core (primarily inorganic) ratio was calculated by dividing the inorganic core area by the organic coating area.

Individual particles were analyzed by Raman microspectroscopy using a Horiba Scientific Labram HR Evolution spectrometer coupled with a confocal optical microscope (100× numerical aperture (N.A.) 0.9 Olympus objective), Nd:YAG laser (50 mW, 532 nm), and CCD detector using a 600 groove mm^{-1} diffraction grating. Individual particle Raman spectra were collected over the 550−4000 cm^{-1} range, with a spectral resolution of ~1.8 cm^{-1}, according to a previously established method.[72] Raman spectra of 88 submicron (0.32− 0.56 μm d_a stage) and 212 supermicron (1.0−1.8 μm d_a stage) sampled SSA particles, identified based on morphology using the optical microscope, were compared to Raman spectra of ~50 standard organic compounds (Table S4), including saccharides, short-chain fatty acids, long-chain fatty acids, and amino acids representative of species present in the marine SML.[19] Linear combinations of up to two model Raman spectra (e.g., 69% galactose + 31% succinic acid) were fitted to ambient SSA Raman spectra following the method of Cochran et al.[19] Therefore, each particle spectrum could match to up to two organic compound types, for example, sucrose + fucose (saccharide + saccharide) or galactose + succinic acid (saccharide + short-chain fatty acid). Model linear combinations and ambient SSA spectra were compared by calculating χ^2 values over the 800−1800 and 2600−3600 cm^{-1} ranges. This analysis provides a value between zero (spectra are identical) and one (spectra have no correlation). Particle spectra matching each organic compound type were characterized by unique peaks corresponding to specific organic functional groups in the 850−1650 and 2700−3500 cm^{-1} regions (Table S5).[53] Further discussion of peak assignments and χ^2 best fit analysis is included in the Supporting Information. The organic compounds corresponding to the best χ^2 fit (smallest value) between model linear combinations and the ambient SSA spectrum are reported.

STXM-NEXAFS analysis was conducted on approximately 150 particles total from the 1.0−1.8 and 0.32−0.56 μm size ranges from two periods (January 26 11:00−17:15 AKST and February 26−27 19:45−8:30 AKST). Beamline 5.3.2.2 at the Advanced Light Source at Lawrence Berkeley National Laboratory (Berkeley, CA) was used for STXM-NEXAFS analysis in a He filled chamber (~200 Torr) of individual particles over the carbon K-edge (278−320 eV), following the method of Moffet et al.[73] The pre- and postedge optical densities at the carbon K-edge were used to determine the inorganic and organic portions of particles.[73] X-ray absorption at 288.6 eV, corresponding to the −COOH functional group,

served as an indicator of organic carbon.[73] The thicknesses of inorganic (NaCl) and organic portions were determined using the optical densities, calculated atomic cross sections for organic (adipic acid) and inorganic (sodium chloride) components, and assumed densities (ρ_{OC} = 1.35 g cm^{-3}, ρ_{NaCl} = 2.16 g cm^{-3}).[18] The organic volume fraction for each particle was calculated as the thickness of the organic portion over the total thickness of organic and inorganic portions.[18,55]

Safety Statement. No unexpected or unusually high safety hazards were encountered in this work.

■ ASSOCIATED CONTENT

ⓢ Supporting Information

The Supporting Information is available free of charge on the ACS Publications website at DOI: 10.1021/acscents-ci.9b00541.

> Additional description of methods; additional discussion of SSA particle, surface snow, and frost flower composition comparisons; Raman spectra peak assignments; determination of organic coating thicknesses; and additional figures including digital color histograms, coastal radar images, S/Na and Mg/Na mole ratios, TEM image, EDX spectra, optical images, fluorescence maps, Raman spectra, SEM images, and size distributions (PDF)

■ AUTHOR INFORMATION

Corresponding Authors

*Phone: 734-763-2283. E-mail: aulta@umich.edu.
*Phone: 734-763-2871. E-mail: prattka@umich.edu.

ORCID ⓘ

Rachel M. Kirpes: 0000-0002-2998-0108
Andrew P. Ault: 0000-0002-7313-8559
Kerri A. Pratt: 0000-0003-4707-2290

Present Address

[⊥]R.C.M.: Sonoma Technology, Petaluma, California 94954, USA

Notes

The authors declare no competing financial interest.

■ ACKNOWLEDGMENTS

■ REFERENCES

(1) Haine, T. W. N.; Martin, T. The Arctic-Subarctic Sea Ice System Is Entering a Seasonal Regime: Implications for Future Arctic Amplification. *Sci. Rep.* **2017**, *7* (1), 4618.

(2) Struthers, H.; et al. The Effect of Sea Ice Loss on Sea Salt Aerosol Concentrations and the Radiative Balance in the Arctic. *Atmos. Chem. Phys.* **2011**, *11* (7), 3459−3477.

(3) Beitler, J. Record low extent in the Chukchi Sea: Arctic Sea Ice News and Analysis. http://nsidc.org/arcticseaicenews/2017/12/record-low-extent-in-the-chukchi-sea/ (accessed Jun 2, 2018).

(4) Richter-Menge, J. A.; Farrell, S. L. Arctic Sea Ice Conditions in Spring 2009−2013 Prior to Melt. *Geophys. Res. Lett.* **2013**, *40* (22), 5888−5893.

(5) Quinn, P. K.; et al. A 3-Year Record of Simultaneously Measured Aerosol Chemical and Optical Properties at Barrow, Alaska. *Journal of Geophysical Research: Atmospheres* **2002**, *107* (D11), AAC8-1−AAC8-15.

(6) Kirpes, R. M.; et al. Secondary Sulfate Is Internally Mixed with Sea Spray Aerosol and Organic Aerosol in the Winter Arctic. *Atmos. Chem. Phys.* **2018**, *18* (6), 3937−3949.

(7) May, N. W.; Quinn, P. K.; McNamara, S. M.; Pratt, K. A. Multiyear Study of the Dependence of Sea Salt Aerosol on Wind Speed and Sea Ice Conditions in the Coastal Arctic. *Journal of Geophysical Research* **2016**, *121* (15), 9208−9219.

(8) Quinn, P. K.; et al. Contribution of Sea Surface Carbon Pool to Organic Matter Enrichment in Sea Spray Aerosol. *Nat. Geosci.* **2014**, *7* (3), 228−232.

(9) Ault, A. P.; et al. Size-Dependent Changes in Sea Spray Aerosol Composition and Properties with Different Seawater Conditions. *Environ. Sci. Technol.* **2013**, *47* (11), 5603−5612.

(10) Ardyna, M.; et al. Recent Arctic Ocean Sea Ice Loss Triggers Novel Fall Phytoplankton Blooms. *Geophys. Res. Lett.* **2014**, *41* (17), 6207−6212.

(11) Quinn, P. K.; Collins, D. B.; Grassian, V. H.; Prather, K. A.; Bates, T. S. Chemistry and Related Properties of Freshly Emitted Sea Spray Aerosol. *Chem. Rev.* **2015**, *115* (10), 4383−4399.

(12) Nilsson, E. D.; et al. Turbulent Aerosol Fluxes over the Arctic Ocean 2. Wind-Driven Sources from the Sea. *Journal of Geophysical Research Atmospheres* **2001**, *106* (D23), 32139−32154.

(13) Leck, C.; Norman, M.; Bigg, E. K.; Hillamo, R. Chemical Composition and Sources of the High Arctic Aerosol Relevant for Cloud Formation. *J. Geophys. Res.* **2002**, *107* (12), 4135.

(14) Scott, W. D.; Levin, Z. E. V. Open Channels in Sea Ice (Leads) as Ion Sources. *Science* **1972**, *177* (4047), 425−426.

(15) Facchini, M. C.; et al. Primary Submicron Marine Aerosol Dominated by Insoluble Organic Colloids and Aggregates. *Geophys. Res. Lett.* **2008**, *35* (17), L17814.

(16) Ault, A. P.; et al. Heterogeneous Reactivity of Nitric Acid with Nascent Sea Spray Aerosol: Large Differences Observed between and within Individual Particles. *J. Phys. Chem. Lett.* **2014**, *5* (15), 2493−2500.

(17) Gord, J. R.; Zhao, X.; Liu, E.; Bertram, T. H.; Nathanson, G. M. Control of Interfacial Cl_2 and N_2O_5 Reactivity by a Zwitterionic Phospholipid in Comparison with Ionic and Uncharged Surfactants. *J. Phys. Chem. A* **2018**, *122* (32), 6593−6604.

(18) Collins, D. B.; et al. Impact of Marine Biogeochemistry on the Chemical Mixing State and Cloud Forming Ability of Nascent Sea Spray Aerosol. *Journal of Geophysical Research Atmospheres* **2013**, *118* (15), 8553−8565.

(19) Cochran, R. E.; et al. Molecular Diversity of Sea Spray Aerosol Particles: Impact of Ocean Biology on Particle Composition and Hygroscopicity. *Chem.* **2017**, *2* (5), 655−667.

(20) Wilson, T. W.; et al. A Marine Biogenic Source of Atmospheric Ice-Nucleating Particles. *Nature* **2015**, *525* (7568), 234−238.

(21) Irish, V. E.; et al. Ice-Nucleating Particles in Canadian Arctic Sea-Surface Microlayer and Bulk Seawater. *Atmos. Chem. Phys.* **2017**, *17* (17), 10583−10595.

(22) Irish, V. E.; et al. Ice Nucleating Particles in the Marine Boundary Layer in the Canadian Arctic during Summer 2014. *Atmos. Chem. Phys.* **2019**, *19* (2), 1027−1039.

(23) Graham, R. M.; et al. Increasing Frequency and Duration of Arctic Winter Warming Events. *Geophys. Res. Lett.* **2017**, *44* (13), 6974−6983.

(24) Hancke, K.; et al. Extreme Low Light Requirement for Algae Growth Underneath Sea Ice: A Case Study From Station Nord, NE Greenland. *Journal of Geophysical Research: Oceans* **2018**, *123* (2), 985−1000.

(25) Assmy, P.; et al. Leads in Arctic Pack Ice Enable Early Phytoplankton Blooms below Snow-Covered Sea Ice. *Sci. Rep.* **2017**, *7*, 40850.

(26) Arrigo, K. R.; et al. Massive Phytoplankton Blooms under Arctic Sea Ice. *Science* **2012**, *336* (6087), 1408.

(27) Mayot, N.; et al. Assessing Phytoplankton Activities in the Seasonal Ice Zone of the Greenland Sea Over an Annual Cycle. *Journal of Geophysical Research: Oceans* **2018**, *123* (11), 8004−8025.

(28) Krembs, C.; Eicken, H.; Junge, K.; Deming, J. W. High Concentrations of Exopolymeric Substances in Arctic Winter Sea Ice: Implications for the Polar Ocean Carbon Cycle and Cryoprotection of Diatoms. *Deep Sea Res., Part I* **2002**, *49* (12), 2163−2181.

(29) Boetius, A.; Anesio, A. M.; Deming, J. W.; Mikucki, J. A.; Rapp, J. Z. Microbial Ecology of the Cryosphere: Sea Ice and Glacial Habitats. *Nat. Rev. Microbiol.* **2015**, *13* (11), 677−690.

(30) Vernet, M.; Matrai, P. A.; Andreassen, I. Synthesis of Particulate and Extracellular Carbon by Phytoplankton at the Marginal Ice Zone in the Barents Sea. *Journal of Geophysical Research: Oceans* **1998**, *103* (C1), 1023−1037.

(31) Leu, E.; et al. Arctic Spring Awakening - Steering Principles behind the Phenology of Vernal Ice Algal Blooms. *Prog. Oceanogr.* **2015**, *139*, 151−170.

(32) Krembs, C.; Eicken, H.; Deming, J. W. Exopolymer Alteration of Physical Properties of Sea Ice and Implications for Ice Habitability and Biogeochemistry in a Warmer Arctic. *Proc. Natl. Acad. Sci. U. S. A.* **2011**, *108* (9), 3653−3658.

(33) Niemi, A.; Michel, C.; Hille, K.; Poulin, M. Protist Assemblages in Winter Sea Ice: Setting the Stage for the Spring Ice Algal Bloom. *Polar Biol.* **2011**, *34* (12), 1803−1817.

(34) Gao, Q.; Leck, C.; Rauschenberg, C.; Matrai, P. A. On the Chemical Dynamics of Extracellular Polysaccharides in the High Arctic Surface Microlayer. *Ocean Sci.* **2012**, *8* (4), 401−418.

(35) Leck, C.; Gao, Q.; Mashayekhy Rad, F.; Nilsson, U. Size-Resolved Atmospheric Particulate Polysaccharides in the High Summer Arctic. *Atmos. Chem. Phys.* **2013**, *13* (24), 12573−12588.

(36) Wernecke, A.; Kaleschke, L. Lead Detection in Arctic Sea Ice from CryoSat-2: Quality Assessment, Lead Area Fraction and Width Distribution. *Cryosphere* **2015**, *9* (5), 1955−1968.

(37) Hirano, D.; et al. Winter Water Formation in Coastal Polynyas of the Eastern Chukchi Shelf: Pacific and Atlantic Influences. *J. Geophys. Res.: Oceans* **2018**, *123* (8), 5688−5705.

(38) Beitsch, A.; Kaleschke, L.; Kern, S. Investigating High-Resolution AMSR2 Sea Ice Concentrations during the February 2013 Fracture Event in the Beaufort Sea. *Remote Sensing* **2014**, *6* (5), 3841−3856.

(39) Johnson, M.; Eicken, H. Estimating Arctic Sea-Ice Freeze-up and Break-up from the Satellite Record: A Comparison of Different Approaches in the Chukchi and Beaufort Seas. *Elementa: Science of the Anthropocene* **2016**, *4* (2004), 000124.

(40) Pilson, M. E. Q. *An Introduction to the Chemistry of the Sea*; Cambridge University Press, 2013; Vol. 51.

(41) Sander, R.; Bottenheim, J. A Compilation of Tropospheric Measurements of Gas-Phase and Aerosol Chemistry in Polar Regions. *Earth System Science Data* **2012**, *4* (1), 215−282.

(42) Yang, X.; Pyle, J. A.; Cox, R. A. Sea Salt Aerosol Production and Bromine Release: Role of Snow on Sea Ice. *Geophys. Res. Lett.* **2008**, *35* (16), L16815.

(43) Kaleschke, L. Frost Flowers on Sea Ice as a Source of Sea Salt and Their Influence on Tropospheric Halogen Chemistry. *Geophys. Res. Lett.* **2004**, *31* (16), L16114.

(44) Douglas, T. A.; et al. Frost Flowers Growing in the Arctic Ocean-Atmosphere-Sea Ice-Snow Interface: 1. Chemical Composition. *Journal of Geophysical Research Atmospheres* **2012**, *117* (3), D00R09.

(45) Jacobi, H. W.; Voisin, D.; Jaffrezo, J. L.; Cozic, J.; Douglas, T. A. Chemical Composition of the Snowpack during the OASIS Spring Campaign 2009 at Barrow, Alaska. *Journal of Geophysical Research Atmospheres* **2012**, *117* (5), 1−13.

(46) Wagenbach, D.; et al. Sea-Salt Aerosol in Coastal Antarctic Regions. *Journal of Geophysical Research: Atmospheres* **1998**, *103* (D9), 10961−10974.

(47) Roscoe, H. K.; et al. Frost Flowers in the Laboratory: Growth, Characteristics, Aerosol, and the Underlying Sea Ice. *J. Geophys. Res.* **2011**, *116* (D12), D12301.

(48) Yang, X.; et al. Evaporating Brine from Frost Flowers with Electron Microscopy and Implications for Atmospheric Chemistry and Sea-Salt Aerosol Formation. *Atmos. Chem. Phys.* **2017**, *17* (10), 6291−6303.

(49) Orellana, M. V.; Leck, C. Marine Microgels. *Biogeochemistry of Marine Dissolved Organic Matter: Second Edition* **2015**, *4*, 451−480.

(50) Jayarathne, T.; et al. Enrichment of Saccharides and Divalent Cations in Sea Spray Aerosol during Two Phytoplankton Blooms. *Environ. Sci. Technol.* **2016**, *50* (21), 11511−11520.

(51) Hawkins, L. N.; Russell, L. M. Polysaccharides, Proteins, and Phytoplankton Fragments: Four Chemically Distinct Types of Marine Primary Organic Aerosol Classified by Single Particle Spectromicroscopy. *Advances in Meteorology* **2010**, *2010*, 1−14.

(52) Shaw, P. M.; Russell, L. M.; Jefferson, A.; Quinn, P. K. Arctic Organic Aerosol Measurements Show Particles from Mixed Combustion in Spring Haze and from Frost Flowers in Winter. *Geophys. Res. Lett.* **2010**, *37* (10), L10803.

(53) Eom, H. J.; et al. Single-Particle Investigation of Summertime and Wintertime Antarctic Sea Spray Aerosols Using Low-Z Particle EPMA, Raman Microspectrometry, and ATR-FTIR Imaging Techniques. *Atmos. Chem. Phys.* **2016**, *16* (21), 13823−13836.

(54) Orellana, M. V.; et al. Marine Microgels as a Source of Cloud Condensation Nuclei in the High Arctic. *Proc. Natl. Acad. Sci. U. S. A.* **2011**, *108* (33), 13612−13617.

(55) Pham, D. Q.; et al. Biological Impacts on Carbon Speciation and Morphology of Sea Spray Aerosol. *ACS Earth and Space Chemistry* **2017**, *1* (9), 551−561.

(56) Gunsch, M. J.; et al. Contributions of Transported Prudhoe Bay Oil Field Emissions to the Aerosol Population in Utqiaġvik, Alaska. *Atmos. Chem. Phys.* **2017**, *17* (17), 10879−10892.

(57) Fu, P.; et al. Fluorescent Water-Soluble Organic Aerosols in the High Arctic Atmosphere. *Sci. Rep.* **2015**, *5*, 9845.

(58) Russell, L. M.; Hawkins, L. N.; Frossard, A. A.; Quinn, P. K.; Bates, T. S. Carbohydrate-like Composition of Submicron Atmospheric Particles and Their Production from Ocean Bubble Bursting. *Proc. Natl. Acad. Sci. U. S. A.* **2010**, *107* (15), 6652−6657.

(59) Frossard, A. A.; et al. Sources and Composition of Submicron Organic Mass in Marine Aerosol Particles. *Journal of Geophysical Research Atmospheres* **2014**, *119* (22), 12977−13003.

(60) Fu, P. Q.; Kawamura, K.; Chen, J.; Charrière, B.; Sempéré, R. Organic Molecular Composition of Marine Aerosols over the Arctic Ocean in Summer: Contributions of Primary Emission and Secondary Aerosol Formation. *Biogeosciences* **2013**, *10* (2), 653−667.

(61) Matrai, P. A.; Tranvik, L.; Leck, C.; Knulst, J. C. Are High Arctic Surface Microlayers a Potential Source of Aerosol Organic Precursors? *Mar. Chem.* **2008**, *108* (1−2), 109−122.

(62) Mashayekhy Rad, F.; Leck, C.; Ilag, L. L.; Nilsson, U. Investigation of Ultrahigh-Performance Liquid Chromatography/ Travelling-Wave Ion Mobility/Time-of-Flight Mass Spectrometry for Fast Profiling of Fatty Acids in the High Arctic Sea Surface Microlayer. *Rapid Commun. Mass Spectrom.* **2018**, *32* (12), 942−950.

(63) Fu, P.; Kawamura, K.; Barrie, L. A. Photochemical and Other Sources of Organic Compounds in the Canadian High Arctic Aerosol Pollution during Winter-Spring. *Environ. Sci. Technol.* **2009**, *43* (2), 286−292.

(64) Scalabrin, E.; et al. Amino Acids in Arctic Aerosols. *Atmos. Chem. Phys.* **2012**, *12* (21), 10453−10463.

(65) Mashayekhy Rad, F.; et al. Measurements of Atmospheric Proteinaceous Aerosol in the Arctic Using a Selective UHPLC/ESI-MS/MS Strategy. *J. Am. Soc. Mass Spectrom.* **2019**, *30* (1), 161−173.

(66) Lovejoy, C.; et al. Distribution, Phylogeny, and Growth of Cold-Adapted Picoprasinophytes in Arctic Seas. *J. Phycol.* **2007**, *43* (1), 78−89.

(67) Law, K. S.; Stohl, A. Arctic Air Pollution: Origins and Impacts. *Science* **2007**, *315* (5818), 1537−1540.

(68) Mauritsen, T.; et al. An Arctic CCN-Limited Cloud-Aerosol Regime. *Atmos. Chem. Phys.* **2011**, *11* (1), 165−173.

(69) Walden, V. P.; Rowe, P. M.; Shupe, M. D.; Cox, C. J. Humidity Trends Imply Increased Sensitivity to Clouds in a Warming Arctic. *Nat. Commun.* **2015**, *6*, 1−8.

(70) Laskin, A.; Cowin, J. P.; Iedema, M. J. Analysis of Individual Environmental Particles Using Modern Methods of Electron Microscopy and X-Ray Microanalysis. *J. Electron Spectrosc. Relat. Phenom.* **2006**, *150* (2−3), 260−274.

(71) Ault, A. P.; et al. Single-Particle SEM-EDX Analysis of Iron-Containing Coarse Particulate Matter in an Urban Environment: Sources and Distribution of Iron within Cleveland, Ohio. *Environ. Sci. Technol.* **2012**, *46* (8), 4331−4339.

(72) Craig, R. L.; Bondy, A. L.; Ault, A. P. Computer-Controlled Raman Microspectroscopy (CC-Raman): A Method for the Rapid Characterization of Individual Atmospheric Aerosol Particles. *Aerosol Sci. Technol.* **2017**, *51* (9), 1099−1112.

(73) Moffet, R. C.; Henn, T.; Laskin, A.; Gilles, M. K. Automated Chemical Analysis of Internally Mixed Aerosol Particles Using X-Ray Spectromicroscopy at the Carbon K-Edge. *Anal. Chem.* **2010**, *82* (19), 7906−7914.